inter.noise
27-30 AUGUST HONG KONG 2017

Retrieving complex surface impedances from statistical absorption coefficients

Boris MONDET[1]; Jonas BRUNSKOG[2]; Cheol-Ho JEONG[3]; Jens Holger RINDEL[4]

[1,2,3] Acoustic Technology, DTU Electrical Engineering, Technical University of Denmark

[1,4] Odeon A/S, Scion-DTU, Denmark

ABSTRACT

In room acoustic simulations the surface materials are commonly represented with energy parameters, such as the absorption and scattering coefficients, which do not carry phase information. This paper presents a method to transform statistical absorption coefficients into complex surface impedances which are needed for phased or time-domain calculation methods. An impedance model based on fractional calculus is suggested to achieve a general model for common acoustic materials. The parameters governing the model are determined by solving an optimisation problem, with constraints ensuring that the impedance found has a physical meaning and respects causality in the time domain. Known material models, such as Miki's and Maa's models, are taken as references to assess the validity of the suggested model. Due to the non-uniqueness of retrieving complex-valued impedances from real-valued absorption coefficients, prior information about the absorber of interest can be used as constraints, which is shown to help determine the correct impedance from absorption coefficient. Further stability and sensitivity investigations indicate that the method presented constitutes an efficient solution to convert sound absorption coefficients back to their original complex surface impedances.

Keywords: Phase retrieval, Surface impedance, Absorption coefficient
I-INCE Classification of Subjects Number: 76

1. INTRODUCTION

Room acoustic simulations have seen a great development in the last thirty years, and nowadays they are used worldwide by acoustic practitioners to predict the behaviours of newly designed renovated rooms. Current software offering room acoustic simulations are based on geometrical acoustics, a high-frequency approximation yielding accurate results above Schroeder's frequency with relatively short computation times. However, problems arise at low frequencies or in small rooms: assumptions behind geometrical acoustics do not hold due to the low modal density, and traditional wave-based methods, such as boundary or finite element methods (BEM, FEM), finite volume method (FVM), or finite difference in the time domain (FDTD), are too time-consuming for practical applications. A possible solution would be to create a hybrid method combining the speed of geometrical acoustics and the accuracy of wave-based methods. Such a hybridization requires an adequate yet different description of the boundary conditions. Indeed, geometrical acoustics only requires energy parameters like absorption and scattering coefficients, which are widely available, whereas wave-based methods need a phased representation of the boundary with complex surface impedances or pressure reflection coefficients. These phased representations are not available for most of the materials encountered in room acoustics, according to ISO 10534 (1) it is only possible to measure such quantities for normal incidence. A compromised solution would be to retrieve the surface impedance from statistical absorption coefficient, which is the main aim of the present paper.

[1] bojmo@elektro.dtu.dk
[2] jbr@elektro.dtu.dk
[3] chj@elektro.dtu.dk
[4] jhr@odeon.dk

2. CURRENT BOUNDARY REPRESENTATION

2.1 Statistical absorption coefficient

In 1982, Thomasson (2) defined three different absorption coefficients: the statistical absorption coefficient, its approximated version, and the alternative absorption coefficient. The method presented in this paper aims at transforming absorption coefficients, which are assumed to have been measured in reverberation chambers. The statistical absorption coefficient is thus considered; for a given frequency, it can be expressed as

$$\alpha_s = 8 \int_0^{\pi/2} \frac{\mathrm{Re}\big(Z_a(\theta)\big)\sin\theta}{|Z_a(\theta) + Z_r(\theta)|^2} d\theta \tag{1}$$

where θ is the incidence angle of the sound wave, Z_a is the surface impedance of the material, and $Z_r(\theta)$ is the radiation impedance of the sample studied. All the acoustic impedances expressed in this paper are normalized by the characteristic impedance of air $\rho_0 c_0$. Thomasson (2), Rindel (3), and Davy et al. (4) successively proposed formulas for the radiation impedance, with Davy et al. being the only ones to suggest a unique formula for all frequencies yielding a complex impedance. For a rectangular sample, and assuming that the speed of sound is larger in the material studied than in air, it can be calculated with equations (53-63) from reference (4). In addition to the incidence angle, it should be noted that the radiation impedance is also dependent on the size of the sample; for an infinite sample, its value tends to $1/\cos\theta$. The international standard for reverberation chamber measurements (5) recommends relatively square samples with areas between 10 m^2 and 12 m^2. Therefore, in this study, it is assumed that all the samples have a square shape and an area of 11 m^2.

2.2 From absorption coefficient to surface impedance

The surface impedance is the ratio of sound pressure and particle velocity at a boundary. It can be decomposed into resistance and reactance, corresponding respectively to the real and imaginary parts. This quantity alone is assumed to be enough to give a complete representation of the boundary. The surface impedance is related to the pressure reflection coefficient by the formula

$$R(\theta) = \frac{Z_a(\theta) - Z_r(\theta)}{Z_a(\theta) + Z_r(\theta)}, \tag{2}$$

and to the statistical absorption coefficient by equation (1). Nevertheless, some conditions have to be respected to ensure that the surface impedance is physically feasible, as explained by Rienstra (6). If the boundary is a passive system it cannot give any energy to the sound wave, then the resistance must be positive:

$$\mathrm{Re}\big(Z_a(\omega)\big) \geq 0 \quad \text{for all } \omega \in \mathbb{R}, \tag{3}$$

ω being the angular frequency. The other conditions are related to the time domain surface impedance $z_a(t)$. Like any physical representation, $z_a(t)$ must respect causality. This implies in the frequency domain:

$$Z_a(\omega) \text{ analytic for } \mathrm{Im}(\omega) < 0, \tag{4}$$

with the $e^{j\omega t}$ convention. Moreover, $z_a(t)$ is meant as a real quantity, and thus the following equality must be satisfied for the conjugate of the surface impedance:

$$Z_a^*(\omega) = Z_a(-\omega). \tag{5}$$

Several authors have attempted to retrieve surface impedances from absorption coefficients. In 2011, Rindel (7) modelled three types of sound absorbers as resonant systems: porous absorbers, membranes, and resonators. He notably pointed out the non-uniqueness of solutions when transforming an absorption coefficient into surface impedance by differentiating soft and hard surfaces. An illustration of this non-uniqueness is given in Figure 1, where isolines of the statistical absorption coefficient are plotted as a function of surface impedance for a given *ke*, the product of the wavenumber and the characteristic length of the sample. Because the statistical absorption coefficient is an energy parameter, there is an infinite number of complex surface impedances corresponding to any value it can take, as seen with the almost circular isolines. Therefore, extra information is needed in addition to the absorption coefficient to retrieve the right impedance, such as the frequency dependence and some other constraints. Figure 1 also gives an illustration of the point of maximal absorption coefficient. With some variations according to the value of *ke*, the surface impedance leading to the highest absorption coefficient is approximately $Z_a = 1.6$.

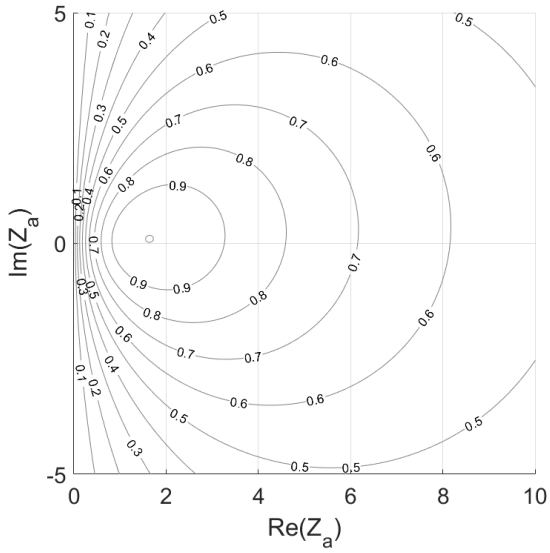

Figure 1 – Iso-absorption coefficient for *ke* = 60 according to Eq. (1)

In 2013, Jeong (8) proposed methods to retrieve the surface impedances of porous absorbers with rigid and air cavity backings as well as fabrics with air cavities. His methods were based on Miki's model and the determination of the flow resistances of the absorbers by solving an optimisation problem, which showed a good agreement in terms of absorption coefficient. They were later applied to measurement data from a round robin experiment (9,10), resulting in a reduction of the standard deviation in absorption coefficient (11).

2.3 Absorber test cases

Impedance models have been suggested for various materials commonly encountered in room acoustics. Porous absorbers have been described with empirical models for many years, and in this study the model presented by Miki (12) is considered. In the case of porous absorbers backed by an air cavity, a multilayered absorber model is applied (13). Three test cases are modelled with the following values for flow resistivity, thickness and cavity depth: (σ, h, d) = (10, 50, 0), (30, 150, 0), (10, 50, 150) in (kPa.s.m^{-2}, mm, mm). These absorbers are later called 'Soft porous', 'Hard porous', and 'Porous with cavity'.

When a porous absorber is covered with a tight membrane, may it be fabric or a thin hard material, the mass and resistance of the membrane affect the surface impedance as explained by Cox and D'Antonio (13). Values for the quantities governing the membrane absorber are estimated to represent an aluminum plate covering a cavity filled with a porous material. The thickness of the plate is set to 5 mm and the cavity depth to 100 mm. The flow resistivity of the porous filling is 75 kPa.s.m^{-2}, and the density and resistance of the aluminum plate are respectively 2700 kg.m^{-3} and 500 $\rho_0 c_0$.

Resonance absorbers (14) are commonly encountered as perforated panels in front of a porous material backed by an air cavity (15). Let us consider a 16-mm-thick panel with a perforation radius of 4 mm, and a perforation rate of 20%. The thickness of the porous material is 40 mm and the depth of the air cavity is 160 mm.

Microperforated panel absorbers have been described by Maa in 1998 (16). The test case for this type of absorbers is given dimensions commonly found in commercial products: the panel thickness is 1 mm, the tube radius is 0.05 mm, the perforation rate is 3%, and the cavity depth is 20 mm.

These different material models are taken as references to validate the impedances retrieved with the method presented in this paper. The surface impedances of the test cases are shown in Figure 2, where clear differences appear between the types of absorbers. The surface impedances of the membrane absorber and the microperforated panel lie where resistance is greater than the point of maximum absorption coefficient. The surface reactance of the membrane absorber is also always positive, with the surface impedance following the curve of an isoline at high frequencies. In the case of the microperforated panel, the surface reactance is negative at low frequencies but increases to positive values with frequency. Regarding the porous absorbers and the perforated panel, their surface impedances lie near the point of maximum absorption coefficient, sometimes with greater values and sometimes with lower values for their resistances and reactances. The effect of the air cavity can be

easily seen with the loops observed in the curves for the porous absorber with cavity and the perforated panel.

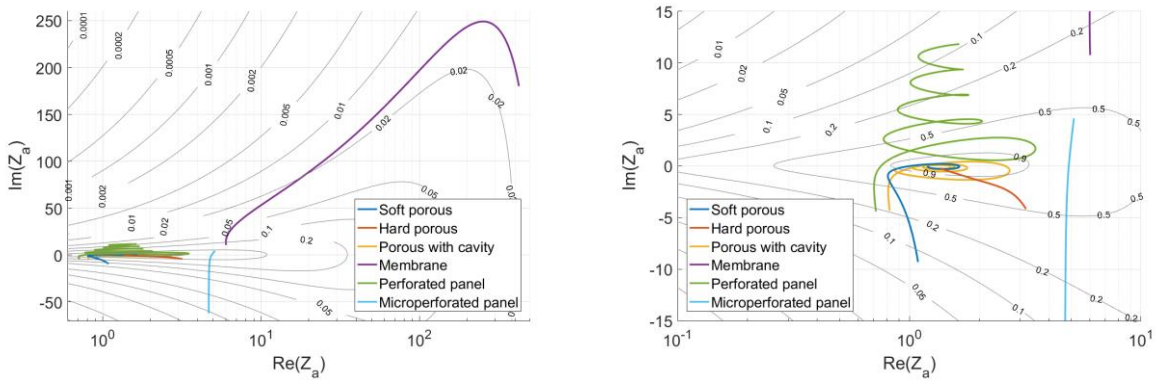

a) Wide view b) Close-up

Figure 2 – Surface impedances of the test cases

3. IMPEDANCE RETRIEVAL METHOD

3.1 Possible general impedance models

In order to represent the different surface materials encountered in room acoustics, several models have been considered as general impedance models, with different levels of complexity. Local reaction is assumed, meaning that the surface impedance is constant over the surface of the sample and over the incidence angles. The models are of two types: a constant term to which are added fractional terms, or a spring-mass-damper model to which are also added fractional terms. The different models are displayed in Table 1. All the parameters are set constant, with $R, M, K, A, B, G \geq 0$, $0 \leq \alpha, \beta \leq 1$, and $-1 \leq \gamma \leq 1$. A fractional derivative (positive γ) or integral (negative γ) can be written

$$(j\omega)^{\gamma} = \cos(\gamma\pi/2)\omega^{\gamma} + j\sin(\gamma\pi/2)\omega^{\gamma} \ . \quad (6)$$

R, *M* and *K* represent the classical resistance, mass and stiffness terms, whereas *A* and *B* correspond to intermediate behaviours between them, typically found in porous and elastic materials, respectively. They indeed consist of a real and an imaginary part; hence, they contribute to both the resistance and the reactance of the surface impedance. Especially, they allow the real part of the surface impedance to be frequency dependent. Finally, *G* is equivalent to either *A* or *B* depending on the sign of γ.

Table 1 – Possible general models for surface impedance

Parameters	Name	Formula	
3	RMK	$Z_a(\omega) = K \cdot (j\omega)^{-1} + R + M \cdot (j\omega)^{1}$	(7)
	R+1	$Z_a(\omega) = R + G \cdot (j\omega)^{\gamma}$	(8)
5	RMK+1	$Z_a(\omega) = K \cdot (j\omega)^{-1} + R + G \cdot (j\omega)^{\gamma} + M \cdot (j\omega)^{1}$	(9)
	R+2	$Z_a(\omega) = A \cdot (j\omega)^{-\alpha} + R + B \cdot (j\omega)^{\beta}$	(10)
7	RMK+2	$Z_a(\omega) = K \cdot (j\omega)^{-1} + A \cdot (j\omega)^{-\alpha} + R + B \cdot (j\omega)^{\beta} + M(j\omega)^{1}$	(11)
	R+3	$Z_a(\omega) = A \cdot (j\omega)^{-\alpha} + R + G \cdot (j\omega)^{\gamma} + B \cdot (j\omega)^{\beta}$	(12)

3.2 Optimisation problem for direct impedance solving

The first step to find a general impedance model is to ensure that the models proposed in Table 1 are capable of representing the surface impedances of a broad range of typical building materials. This is performed through direct impedance solving: after creating an input impedance for each of the test cases described previously, the parameters of the possible general models are determined by minimizing the L2-norm between the input and output impedances. The cost function to be minimized is

$$F_Z = \sum_i \|Z_{in}(f_i) - Z_a(f_i)\|_2^2 \ , \tag{13}$$

where Z_{in} and Z_a are respectively the input and modelled impedances, and f_i are the centre frequencies of the 1/3-octave bands between 100 Hz and 5000 Hz. No constraints are applied to this optimisation problem, and MATLAB solver *fmincon* is used to handle the problem. When the test case chosen for optimisation is extendedly reacting, the input impedance is taken equal to the surface impedance for an incidence angle of $\pi/4$, as an approximation of the surface impedance under diffuse incidence (17). The starting point of the optimisation is chosen near to the point of maximal absorption coefficient, i.e. $Z_{start}(f_i) = 1.6$.

The goodness of the fit for the optimal impedances to the input impedances is then assessed with the adjusted R^2. This quantity allows to take into account the number of parameters and indicates whether or not additional parameters bring new information to the model. It is calculated from the R^2 value as follows:

$$R^2_{adj} = 1 - \frac{(1-R^2)(n-1)}{n-q-1} \ , \tag{14}$$

where n is the number of data points, and q is the number of parameters in the model excluding the constant term. The formula for R^2 makes use of the residual and total sums of squares:

$$SS_{res} = \left\| f_{ref} - f_{model} \right\|_2^2 , \tag{15}$$

$$SS_{tot} = \left\| f_{ref} - \overline{f_{ref}} \right\|_2^2 , \tag{16}$$

$$R^2 = 1 - \frac{SS_{res}}{SS_{tot}} = 1 - \frac{MSE}{V_{ref}} \ . \tag{17}$$

f_{ref} represents the reference data points, i.e. the input impedance in the present case, $\overline{f_{ref}}$ is its mean, and f_{model} corresponds to the fitted data points. The ratio between the residual and total sums of squares can also be seen as the ratio between the mean square error *MSE* of the model to the reference and the variance of the reference V_{ref}.

3.3 Optimisation problem for absorption solving

The objective of the present impedance retrieval method is to convert absorption coefficients to surface impedances. Commonly available data for room acoustics materials is the statistical absorption coefficient in octave bands from 125 Hz to 4000 Hz; this is therefore taken as input data to the optimisation problem. The strategy to retrieve the surface impedance is to minimize the difference between the input and the absorption coefficient corresponding to the retrieved impedance. Some constraints are applied to the optimisation in order to ensure that the right impedance is retrieved.

First, general constraints corresponding to the requirements for a physical impedance are set. The retrieved impedance is constrained to have a positive real part as in Eq. (3), while Eq. (4,5) are automatically satisfied with the functions chosen for the models.

Moreover, if the input absorption coefficient is greater than 0.01 in all octave bands, the search range for the impedance is limited to a real part between $0.002\,\rho_0 c_0$ and $1600\,\rho_0 c_0$, and an imaginary part between $-800\,\rho_0 c_0$ and $800\,\rho_0 c_0$; these values correspond to absorption coefficients greater than 0.005.

Besides, some constraints may be applied according to the different absorbers. On one hand, absorbers are considered to be soft when the real part of their surface impedance is close to or lower than that of air. On the other hand, absorbers are considered to be hard when their surface resistance is greater than that of air. Translated into constraints, the resistances of soft and hard materials are forced to be lower than $2\,\rho_0 c_0$ and greater than $1\,\rho_0 c_0$, respectively. The region where the resistance is comprised between $1\,\rho_0 c_0$ and $2\,\rho_0 c_0$ is purposely shared by both absorber types as it coincides with the values yielding the maximal absorption coefficients. Finally, additional constraints are applied in the case of porous materials: the imaginary part of the impedance must be negative, and the real part must be lower than $2\,\rho_0 c_0$ for 2000 Hz and 4000 Hz octave bands.

The whole optimisation problem can be summarized as follows:

$$\min \ F = \sum_{oct} \|\alpha_{in}(f_{oct}) - \alpha_s(f_{oct})\|_2^2 \ ; \tag{18}$$

$$\mathrm{Re}\left(Z_a(f_i)\right) \geq 0 \ ; \tag{19}$$

$$\text{if } \alpha_{in}(f_{oct}) \geq 0.01 \text{ for all } f_{oct} \qquad 0.002 \leq \mathrm{Re}\left(Z_a(f_i)\right) \leq 1600 \ , \tag{20}$$

$$-800 \leq \mathrm{Im}\left(Z_a(f_i)\right) \leq 800\ ; \tag{21}$$

$$\mathrm{Re}\left(Z_a(f_i)\right) \geq 1 \quad \text{or} \quad \mathrm{Re}\left(Z_a(f_i)\right) \leq 2\ ; \tag{22}$$

porous absorbers:

$$\mathrm{Im}\left(Z_a(f_i)\right) \leq 0\ , \tag{23}$$

$$\mathrm{Re}\left(Z_a(f_i)\right) \leq 2 \quad \text{for } 1600 \text{ Hz} \leq f_i \leq 5000 \text{ Hz}\ . \tag{24}$$

In these equations, F is the cost function, α_{in} is the input absorption coefficient, a_s is the statistical absorption coefficient obtained from the retrieved impedance, f_{oct} represents the octave bands between 125 Hz and 4000 Hz, Z_a is the retrieved impedance, and f_i corresponds to the centre frequencies of the 1/3-octave bands between 100 Hz and 5000 Hz. The choice of the constraint in Eq. (22) depends on the absorber under consideration. From Figure 2, it can be inferred that the hardness constraint $\mathrm{Re}\left(Z_a(f_i)\right) \geq 1$ is to be applied to membrane absorbers and microperforated panels, as well as high flow resistivity and thick porous absorbers. Inversely, the softness constraint $\mathrm{Re}\left(Z_a(f_i)\right) \leq 2$ should be applied to perforated panels and thin porous absorbers with low flow resistivity. The starting point of the optimisation is identical to direct impedance solving with $Z_{start}(f_i) = 1.6$. The solutions found by the algorithm are considered valid under one condition:

$$F \leq 0.015 \quad \text{if } a_{in}(f_{oct}) \leq 1 \text{ for all } f_{oct}\ , \tag{25}$$

$$F \leq 0.25 \quad \text{otherwise}\ , \tag{26}$$

which is respectively equivalent to a root-mean-square error of 0.05 and around 0.2 between the input and retrieved absorption coefficients. Cases where the input absorption coefficient is greater than 1 are allowed a larger error because the general models proposed tend to yield values that exceed 1 to a lesser extent than what can be observed in measurements.

4. CONVERSION OF ABSORPTION COEFFICIENTS

4.1 Model selection

The method for direct impedance solving is applied to the test cases given in Section 2.3 with all the possible general models, in order to evaluate how well they can represent the different types of absorbers. The results of the optimisations are gathered in Table 2. It can first be seen that the RMK model performs poorly at reproducing the surface impedance of the membrane absorber, the adjusted R^2 value being even negative. This is not surprising because RMK only presents constant resistances, while the surface resistance of the membrane varies greatly as was seen in Figure 2. The fit of RMK to the surface impedance of the hard porous case is also significantly lower than that of the other models. The same observation can be made for the R+1 model with the perforated panel absorber. These two models can thus be considered inappropriate for a general impedance model. Among the four remaining models, the highest value of adjusted R^2 is found for either the RMK+1 or R+2 models in all the test cases except the hard porous absorber. It indicates that the extra parameters included in the RMK+2 and R+3 models do not bring new information. In addition, the adjusted R^2 values obtained with the RMK+1 and R+2 models are very close if not equal. Therefore, the two models with 5 parameters, RMK+1 and R+2, are the most efficient at representing the surface impedances of various common sound absorbers. Nevertheless, the results presented here do not allow to choose one model over the other; consequently, the two models are selected and their performances will be compared in the later sections.

Table 2 – Adjusted R^2 between input and retrieved impedances

Absorber	RMK	R+1	RMK+1	R+2	RMK+2	R+3
Soft porous	0.9813	0.9782	0.9863	0.9885	0.9864	0.9864
Hard porous	0.6323	0.9925	0.9962	0.9907	0.9971	0.9971
Porous with cavity	0.7256	0.7237	0.7274	0.7274	0.6778	0.6778
Membrane	-0.0709	0.7510	0.7202	0.7202	0.6693	0.6605
Perforated panel	0.9468	0.7872	0.9472	0.9417	0.9376	0.9376
Microperforated panel	0.9999	0.9845	0.9999	0.9999	0.9999	0.9999

Although similar in some aspects, the RMK+1 and R+2 models differ in their physical

interpretation. On one hand, the four terms in the RMK+1 model represent the classical spring-mass-damper system to which either an elastic or a porous behaviour is added. On the other hand, the R+2 model can be seen as a generalization of the RMK model where the fractional terms describe the intermediate behaviours between pure resistance and pure mass or stiffness. The spring-mass-damper system is still included in this model as the extreme case $\alpha = \beta = 1$.

4.2 Performance of the retrieval method

The RMK+1 and R+2 models were showed to be the most efficient general impedance models. However, the goal of this study is to retrieve surface impedances from statistical absorption coefficients. Therefore, the absorption solving method is applied to the same test cases as previously with the two selected models. From the results displayed in Table 3, a very poor fit can be observed for the membrane absorber with both general models. It is mostly due to the behaviour of the membrane input model: at high frequencies, the surface impedance follows the curve of an absorption coefficient isoline (cf. Figure 2). On the contrary, the general models can only yield monotonically increasing reactances, which results in absorption coefficients that keep decreasing at high frequencies. Considering the difficulty to describe membrane absorbers, it is likely that inaccuracies are present in the general and input models. When looking at the other absorbers, it is found that the RMK+1 model performs better for the hard porous absorber and the perforated panel, while the R+2 model shows a better fit with the soft porous absorber. The two models exhibit equivalent performances in the cases of the porous absorber with cavity and the microperforated panel. Overall, the RMK+1 model appears more advantageous than the R+2 model with theoretical input data. In practical applications though, input data consist in measurement results which are affected by noise from various origins. The retrieval method should thus be confronted to measured input data to confirm its validity.

Table 3 – R^2 between input and retrieved impedances

Absorber	RMK+1	R+2
Soft porous	0.6750	0.7814
Hard porous	0.9649	0.8581
Porous with cavity	0.7324	0.7324
Membrane	-1.1286	-1.1283
Perforated panel	0.8432	0.7918
Microperforated panel	0.6247	0.6258

4.3 Impedance retrieval from measured data

In 2009 Tompson and Vercammen led a round robin study on reverberation chambers (9,10). The statistical absorption coefficients of four different samples were measured in 13 laboratories in Europe. The results of this study are taken as input to the retrieval method to assess its sensitivity to the noise and deviations that exist in real measurements. The first sample in the study is a foam material with a flow resistivity estimated to $\sigma \cong 50\,\mathrm{kPa.s.m^{-2}}$ and a thickness $h = 25\,\mathrm{mm}$, to which the hardness constraint is applied for the optimisation. Another porous material was included in the study with a mineral wool sample whose flow resistivity is $\sigma = 19.8\,\mathrm{kPa.s.m^{-2}}$ and thickness $h = 100\,\mathrm{mm}$, categorized as a soft material for the optimisation. The third sample is a membrane absorber consisting of the same mineral wool as the second sample with a 5-mm thick hardboard cover. Finally, the fourth sample is a combination of the previous membrane and mineral wool absorbers, with units arranged in a chessboard pattern. 13 surface impedances are retrieved for each sample, corresponding to the 13 input absorption coefficients.

The normalized standard deviations (STDn) are then compared between the input absorption coefficients and the retrieved absorption coefficients, as shown in Figure 3. The first observation is that the two general impedance models often return similar results. For the two porous absorbers, it can be seen that the absorption coefficients retrieved with RMK+1 and R+2 have lower STDn than the ones measured at almost all frequencies. Only the foam absorber around 250 Hz does not follow this trend. Concerning the combined absorber, the STDn of the retrieved absorption coefficients are very similar to that of the measured ones. The membrane absorber is the only case where significant differences

appear between the two impedance models. Below 400 Hz, both the models and the measured data lead to close STDn. Above 400 Hz, however, the RMK+1 model yields a higher STDn than the measurements, whereas the R+2 model exhibit values close to the measured data and even lower values in the highest octave band.

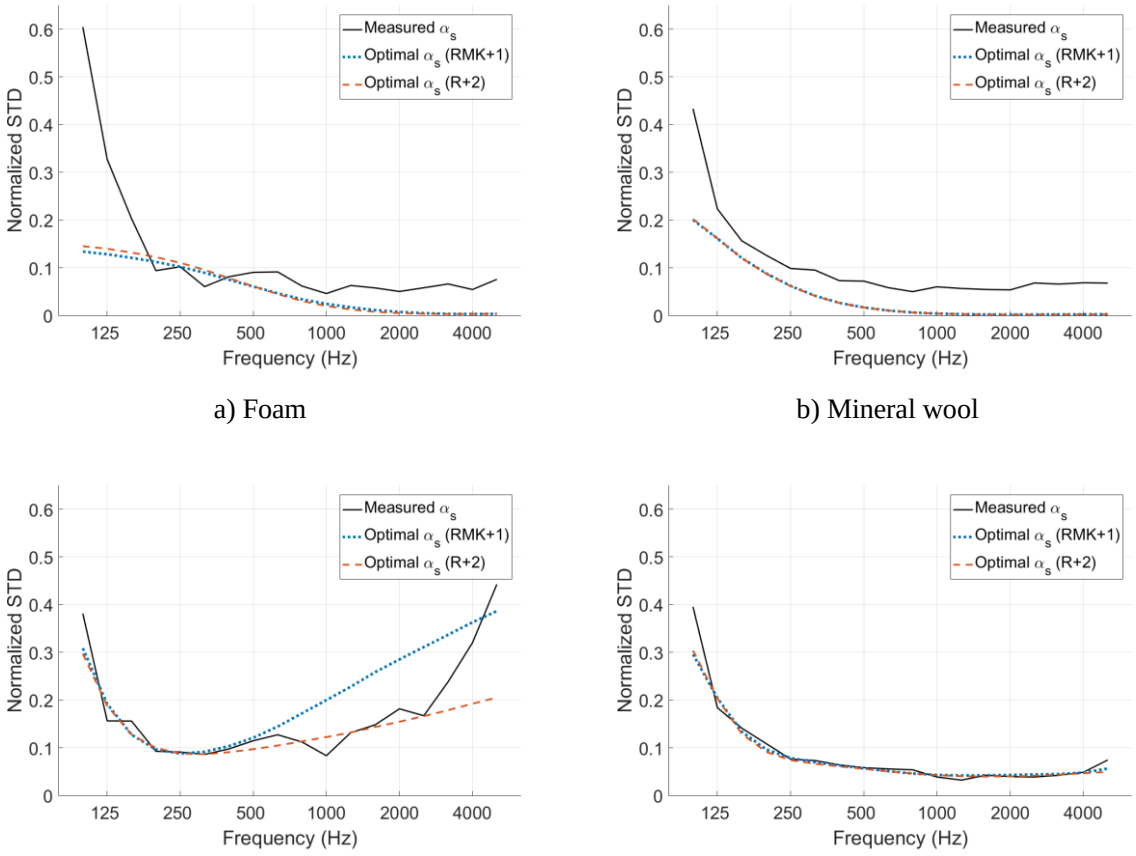

a) Foam

b) Mineral wool

c) Membrane

d) Combination

Figure 3 – Normalized standard deviations of input and retrieved absorption coefficients

Another illustration of these results is displayed in Figure 4, where the standard deviations are represented as ranges in dashed lines along the means of the absorption coefficients in solid lines. The curves corresponding to RMK+1 and R+2 almost always overlap, the only discrepancies appearing in the membrane absorber case and especially at high frequencies. Besides, the retrieved impedances tend to yield lower values of absorption coefficient than the measurements. This is seen with the foam absorber above 500 Hz, with the mineral wool above 160 Hz, and with the membrane absorber above 1600 Hz. The combined absorber is the only case where the results of the retrieval method are similar to the results of the measurements, both in terms of mean value and standard deviation.

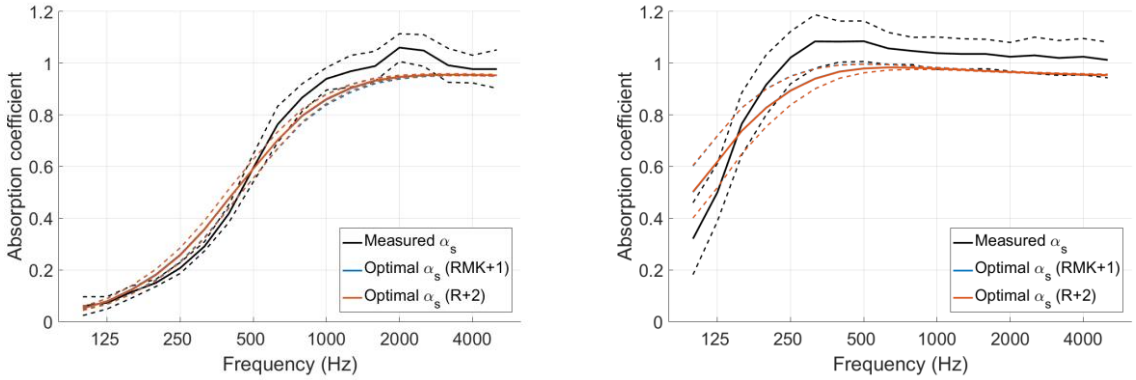

a) Foam

b) Mineral wool

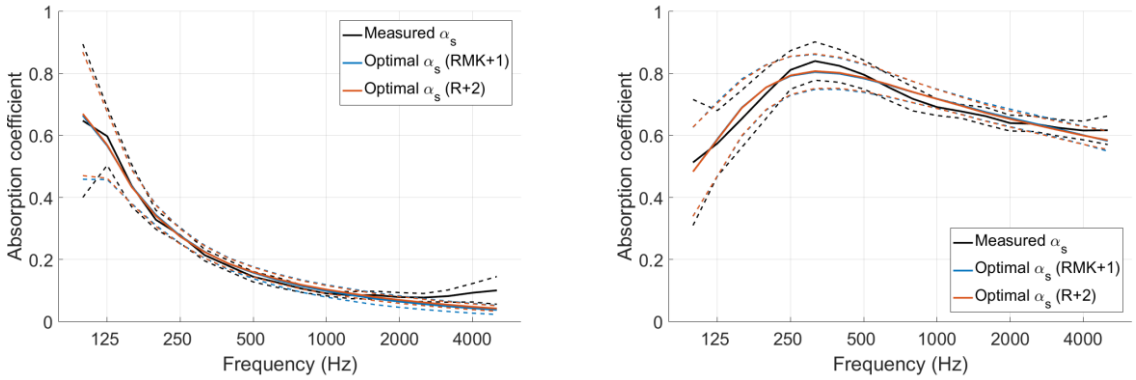

c) Membrane d) Combination

Figure 4 – Absorption coefficients of the different samples. Dashed lines: ± 1 STD

5. DISCUSSION

The general impedance models presented in this paper are based on fractional calculus. The formulas of these models all imply that the imaginary part of the surface impedance is monotonically increasing. While this is a fair assumption in most cases, the theoretical models for the impedances of porous absorbers with cavities and membrane absorbers describe otherwise. Consequently, the performance to retrieve the impedances of such absorbers is limited, as seen already in Table 2 with direct impedance solving. It can lead to even greater discrepancies in absorption solving; it was for example the case with the membrane absorber in Table 3. As a result, the method presented should be applied with caution when retrieving the impedances of these absorbers, whichever general model is selected.

The results of impedance retrieval showed close results between the two models selected in section 4.1. The RMK+1 and R+2 are indeed similar mathematically, even though their physical interpretations differ. From the impedances retrieved in this paper, the R+2 model seems to yield more robust results than the RMK+1 when input data are based on measurements. However, the discrepancies observed are not large enough to completely discard the RMK+1 model, and further investigation is required. It is expected that a stability analysis and the study of transformation to the time domain will bring new clues to decide which of the models is best suited for surface impedance retrieval from statistical absorption coefficients.

One issue not addressed here is the amount of prior information about the sound absorber under study. It is critical to know the type of absorber in order to apply the right constraints, especially for porous absorbers. These absorbers indeed require more specific and restricting constraints than the others. A possible solution would be to implement an automatic material detection with machine-learning: based on the input absorption coefficient, the type of sound absorber would be deduced and the corresponding constraints applied. However, it would require a large amount of training data, which is not necessarily available for all types of sound absorber. Naturally, training data could be created from the theoretical models, but it would not cover all the phenomena taking place in measurements.

6. CONCLUSION

This paper presented a method to retrieve the surface impedances of various sound absorbers from their statistical absorption coefficients. After suggesting several general impedance models based on fractional calculus, a first optimisation problem was set to minimize the difference between those general impedance models and the theoretical impedance models of sound absorber test cases. It was demonstrated that a general surface impedance model could be most efficiently expressed with five parameters. Two general models were thus selected for further study: the RMK+1 and R+2 models. Theoretical absorption coefficients were then calculated, and the parameters of the two models were determined with a second optimisation problem. A good agreement was found between the original surface impedances and those retrieved with RMK+1 and R+2; the only exception was the case of a membrane absorber. The impedance retrieval method was finally applied to the results of a round robin

experiment where the absorption coefficients of four sound absorbers were measured in 13 different reverberation chambers. By retrieving the corresponding surface impedances, it was shown that the absorption coefficients obtained with the R+2 model always had similar or lower standard deviations than the ones measured in the laboratories, even in the case of the membrane absorber. Therefore, the impedance retrieval method presented with the R+2 model appeared to be robust to noisy input data, i.e. to deviations in measured absorption coefficients. Despite these promising results, further investigation is required to confirm the validity of this method, especially with a stability analysis of the optimisation problem. A transformation of the retrieved surface impedances to the time domain will also be implemented for later applications in numerical simulations for room acoustics.

REFERENCES

1. ISO 10534:1998. Acoustics - Determination of sound absorption coefficient and impedance in impedance tubes. International Organization for Standardization. Geneva, Switzerland 1998.
2. Thomasson S-I. Theory and experiments on the sound absorption as function of the area. Report No. TRITA-TAK-8201. Department of Technical Acoustics, Royal Institute of Technology. Stockholm, Sweden 1982.
3. Rindel JH. Modelling the angle-dependent pressure reflection factor. Applied Acoustics. 1993;38:223-234.
4. Davy JL, Larner DJ, Wareing RR, Pearse JR. The average specific forced radiation wave impedance of a finite rectangular panel. J. Acoust. Soc. Am. 2014;136(2):525-536.
5. ISO 354:2003. Acoustics - Measurement of sound absorption in a reverberation room. International Organization for Standardization. Geneva, Switzerland 2003.
6. Rienstra SW. Impedance models in time domain. Messiaen - Project AST3-CT-2003-502938. Deliverable 3.5.1 of Task 3.5. 2005.
7. Rindel JH. An impedance model for estimating the complex reflection factor. Forum Acusticum 2011; 27 June - 1 July 2011; Aalborg, Denmark 2001. CD-ROM.
8. Jeong C-H. Converting Sabine absorption coefficients to random incidence absorption coefficients. J. Acoust. Soc. Am. 2013;133(6):3951-3962.
9. Tompson D, Vercammen M. Research for investigation of absorption measurement deviation. Report No. RA 547-1-BR. Laboratory for Acoustics, Peutz BV. Molenhoek, Netherlands 2009
10. Vercammen M. Improving the accuracy of sound absorption measurement according to ISO 354. ISRA 2010; 29-31 August 2011; Melbourne, Australia 2010. CD-ROM.
11. Jeong C-H, Chang J-H. Reproducibility of the random incidence absorption coefficient converted from the Sabine absorption coefficient. Acta Acustica united with Acustica. 2015;101:99-112.
12. Miki Y. Acoustical properties of porous materials - Modifications of Delany-Bazley models. J. Acous. Soc. Jpn. 1990;11(1):19-24.
13. Cox TJ, D'Antonio P. Porous absorption. In: Cox TJ, D'Antonio P. Acoustic Absorbers and Diffusers: theory, design, and application. 2nd ed. London, UK, and New York, USA: Taylor & Francis; 2009. p. 156-195.
14. Ingard U. On the theory and design of acoustic resonators. J. Acoust. Soc. Am. 1953;25(6):1037-1061
15. Attenborough K, Vér IL. Sound absorbing materials and sound absorbers. In: Vér IL, Beranek LL. Noise and Vibration Control Engineering. 2nd ed. New York, USA: John Wiley & Sons; 2006. p. 215-277
16. Maa DY. Potential of microperforated panel absorber. J. Acoust. Soc. Am. 1998;104(5):2861-2866.
17. Jeong C-H, Brunskog J. The equivalent incidence angle for porous absorbers backed by a hard surface. J. Acoust. Soc. Am. 2013;134(6):4590-4598.